sciendo

POLISH MARITIME RESEARCH 2 (114) 2022 Vol. 29; pp. 43-54
10.2478/pomr-2022-0016

ANALYSIS OF MARINE RISERS SUBJECTED TO SHOAL/DEEP WATER IN THE INSTALLATION PROCESS

Yikun Wang
Songxiang Luo
Mo Yang
Tao Qin*
Jing Zhao
Gang Yu
School of Mechanical Engineering, Hubei University of Arts and Science, China

* Corresponding author: *heu_qt@163.com (T. Qin)*

ABSTRACT

The dynamics of the installation process of marine risers subjected to shoal/deep seawater is studied. The riser is assumed to be a cantilevered Euler–Bernoulli beam. The upper end of the riser is clamped on the vessel or the drilling platform. The lower end of the riser is connected to the Blowout Preventer Stack (BOPs) and Lower Marine Risers Package (LMRP). The lateral fluid forces induced by the sea wave and sea current are introduced into the governing equations of motion. The lateral displacement and stress distributions of the riser are obtained by solving the governing equation of the riser via Galerkin's discretisation scheme and a fourth-order Runge–Kutta algorithm. The results indicate that the riser exhibits different behaviours under various depths because of the different distributions of the flow velocity ranging from the sea surface to the seabed. In the case of shoal water, the dynamics of the riser are dominated by the sea wave, while in the case of deep water it is affected mainly by the sea current velocity and sea surface wind velocity.

Keywords: sail catamaran, green shipping, zero emission, hybrid propulsion

INTRODUCTION

Marine risers have been shown to have importance in ocean engineering, such as the connection between the subsea wellhead and the floating vessel or drilling platform. To maintain the good condition of the riser during its lifetime, correct installation has become more and more important in recent years [1-4]. The cross-flow velocity of the seawater generally consists of three parts, i.e., the sea wave, the sea current, and the sea surface wind [5, 6]. When the riser is in the installation process, it will experience lateral and axial forces in which the former is generated by the cross-sea water and the latter is induced by the gravity of the riser and BOPs/LMRP. The two types of force vary with the depth of the seawater and the length of the riser [7, 8].

A large number of papers on the mechanics of marine risers have been published in the past five decades. Chakrabarti [9] obtained the velocity potential expression in the cylindrical polar coordinate system and determined the dynamic pressure on the surface of the cylinder. The total horizontal wave forces on the cylinder were also determined in an equivalent form of the inertial part of J.R. Morison's equation. The dynamic behaviours of two kinds of marine riser systems were compared by Wang [10]. One is an air can system and the other one is a syntactic foam system, compared under different operating conditions, such as the installation and retrieval, normal weather drilling, heavy weather standby and free-standing storm survival conditions. A computer program was developed by Azpiazu et al. [11] to establish the performance of heave compensator systems under actual at-sea working conditions. The vertical dynamics of marine riser-load systems were studied by Azpiazu and Nguyen [12], in order to determine the amplitude of dynamic forces and displacements caused by heave action. Trim [13] derived the governing equation of axial motion and explored several load cases in practical engineering, which focused mainly on deep

Nomenclature

A_i	inner side area of the riser
A_o	outer side area of the riser
A_r	cross-section area of the riser
C_D	drag coefficient
C_M	inertial coefficient
c	distributed viscous damping coefficient of the riser
D	outer diameter of the riser
d_t	thickness of the riser
E	Young's modulus of the riser
E_k	kinematic energy of the system
E_p	potential energy of the system
$f(x, t)$	distributed lateral force
$f_D(x, t)$	drag force induced by the sea wave and current
$f_I(x, t)$	inertial force induced by the sea wave and current
$f_i(q_j, q_j)$	column vector of the discretised lateral force
g	gravitational acceleration
H	wave height of the sea wave
I	rotational inertia of the riser cross-section
k	wave number of the sea wave
L	length of the riser
L_{all}	total length of the seawater
L_w	wave length of the sea wave
$M_y(x, t)$	bending moment of the riser
m_e	mass of the BOPs/LMRP
N	number of truncating modes
T	wave period of the sea wave
$q_j(t)$	jth generalised coordinate
$T(x)$	axial tension of the riser at position x
t	time variables
v	total velocity of the sum of sea current, surface wind and sea wave
v_c	velocity of the sum of sea current and sea surface wind
v_w	horizontal velocity of the sea wave1
v_1	velocity of the sea surface wind2
v_2	velocity of the sea surface current
W	virtual work done by the lateral force and damping force
x	axis of the horizontal direction
y	axis of the vertical direction
$y(x, t)$	lateral displacement of the riser
ρ_a	density of the seawater
ρ_r	density of the riser
$\varphi_j(x)$	jth eigenfunction of a cantilevered beam
λ_j	jth eigenvalue of a cantilevered beam
σ_{von}	Von Mises stress
$\sigma_1, \sigma_2, \sigma_3$	three principal stresses

water conditions. The results showed that for water depths of several thousand feet or more, the vertical motions and forces following disconnect and during hang off can be large. Two alternatives of the coupling oscillations between axial and lateral vibrations were discussed by Johnson and Roesset [14], in which the possibility of uncoupling the analysis for axial and lateral vibrations is explored. Good results could be provided via the scheme whereby the values of the axial forces resulting from the uncoupled axial analysis at each step are employed for the lateral analysis. Burrows et al. [15] used rigid and flexible forms of the Morison equation to determine the drag and inertial force under random wave excitation. They found that, for nondeterministic analyses, Morison's equation reproduces well the probability distribution of loading associated with given sea state conditions. A detailed illustration of the determination of drag and inertial force coefficients was presented. The differential equation was derived by Moe and Larsen [16] to describe the motions of a marine riser with an asymptotic solution, in which the riser is subjected to wave forms travelling away from the excited zone. Possible causes for the unexpected large discrepancies are discussed in the analyses. Kogure et al. [17] proposed several operational aspects to ensure the safety of marine risers in deep water, mainly concerning the time required to pull the drilling riser in the case of an emergency. For more details, the interested reader can refer to the review article related to marine risers [18].

In the early 21st century, another wave of researchers conducted studies on the dynamics of marine risers from new aspects that may occur in practical engineering. For instance, the variation approach was presented to explore the two-dimensional large strain static mechanics of marine risers [19]. Strain energy due to bending and axial stretching, virtual work induced by hydrostatic pressures and other external forces were involved in the governing equation. Yazdchi and Crisfield [20] considered the full three-dimensional analysis of pipes in which bending stiffness was included. The equation of three-dimensional oscillation of marine risers was formulated in the case of large elastic deflections using Kane's formalism [21]. Mathelin and de Langre [22] explored the vortex-induced vibration based on a wake oscillator model, and theoretical analysis was conducted to predict the wave-packets' amplitude and distribution. A finite difference method was proposed to address the dynamic equilibrium problem of 2D marine risers by Chatjigeorgiou [23] and particular attention was given to the transversal motions and the associated bending moments. Dai et al. [24] focused on the global analysis of drilling risers, which includes two aspects: an operability analysis and a hang-off analysis used to check the design of the risers. The flexible risers were modelled as slender elastic structures by Santillan et al. [25]. The nonlinear boundary value problem was illustrated, which can be solved numerically with appropriate boundary conditions. A new method was proposed to suppress the riser's vibration by using two actuators in the transverse and longitudinal directions [26]. The control problem of a marine riser during the installation process was studied [27]. Based on Lyapunov's direct method, the top and bottom boundaries were adapted to position the subsea payload to the desired set point and suppress the riser's vibration. A time-domain analysis tool was developed to predict the vortex-induced vibration of marine risers based on a forcing algorithm [28].

The above-mentioned studies are related to marine risers that have been connected to a subsea wellhead. Influences

generated from the fluid around the risers are also important in the investigation of the dynamics in its installation, such as the damping effect, impact between the risers and coupled vibrations of the axial and lateral direction. The differential equation for axial vibration was deduced in [29] by considering the influence of damping on the vibration in its installation. A static analysis was conducted to analyse the lateral displacement, deformation and stress in its installation [30, 31]. The effects of vessel motion and movement of the sea wave were involved. Hu et al. [32] obtained the static lateral displacement and Von Mises stress of the riser in its installation through numerical simulation. Chang et al. [33] investigated the in-line and cross-flow coupling vibration response characteristics of a marine viscoelastic riser subjected to two-phase internal flow. The numerical results demonstrated that appropriate viscoelastic coefficients are very important to effectively suppress the maximum displacements and stresses of the risers. Liu et al. [34] studied the dynamics of cross-flow tubes in consideration of initial axial load and distributed impacting constraints. The bifurcation diagrams were constructed in relation to boundary conditions and structural parameters. Buckling, fluttering and chaotic oscillating are observed from the numerical calculations.

The purpose of this paper is to investigate the dynamics during the installation process of marine risers subjected to shoal/deep seawater. The aforementioned works focused either on the case of shoal water or on deep water in which the water depth is ideally assumed to be equal to the length of the riser. In this paper, the depth of the seawater is fixed to be 1500 m. Shoal water should be in the range of 0 m to 200 m, and the depth of deep water is greater than 200 m. In the installation process, the riser will penetrate from shoal water to deep water, such that the flow velocity of the seawater at the bottom of the riser is not zero unless the riser reaches the seabed. From this point of view, the definition of shoal water and deep water in this paper is different from the foregoing research. Wang et al. [31] have proved that the actual riser vibration response is the linear superposition of the vessel motion and riser lateral vibration under the action of the sea wave and current. Thus, for simplicity in this paper, the vessel or the drilling platform is assumed to be a fixed platform. The riser is regarded as a cantilevered Euler–Bernoulli beam. The upper end of the riser is clamped onto the vessel or the drilling platform, and the lower end of the riser is connected to the BOPs/LMRP. The lateral displacement and stress distributions of the riser will be obtained by solving the governing equation of the riser via Galerkin's discretisation scheme and a fourth-order Runge–Kutta algorithm.

MODEL DESCRIPTION

We assume that the vessel or drilling platform has no horizontal and longitudinal vibration [31]. The top of the riser is clamped onto the vessel or the drilling platform. The Euler–Bernoulli beam theory is adopted. The riser has constant density and a uniform cross-section. The BOPs/LMRP at the free end of the riser are considered as mass blocks. The lateral force by the sea wave and sea current is distributed along the riser axis. The axial tension force is induced by the self-weight of the riser and BOPs/LMRP, and buoyancy force in the installation process. The lateral force imposed on the riser is generated by the sea wave and sea current. It should be mentioned that, during the calculation process, the fluid forces are neglected initially and the length of the riser extends quasi-statically. When the length of the riser reaches the corresponding stages, as shown in Fig. 1, the fluid forces will be activated immediately.

The clamped end is taken as the origin of the coordinate, the gravity direction as the axis and the direction of current flow as the axis. The four stages of the risers in the installation are presented. Stage 1 reflects the shoal water of the riser in the installation, stages 2 and 3 are the transition from the shoal water to deep water and stage 4 involves the riser completing its installation and reaching the seabed.

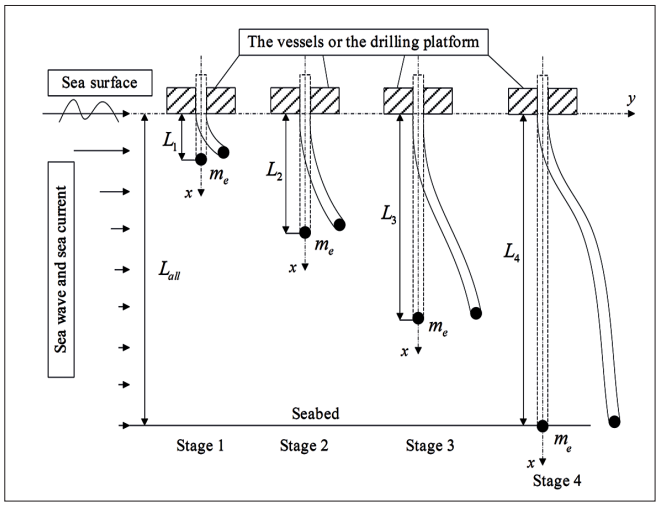

Fig. 1. Schematic diagram of the riser in the installation process

The governing equation of the riser will be derived through a variation approach. The kinematic energy E_k of the system is given by

$$E_k = \int_0^L \frac{1}{2} (\rho_r A_r + \rho_a A_i)\left(\frac{\partial y}{\partial t}\right)^2 dx, \tag{1}$$

where L is the length of the riser, ρ_r and ρ_a are the density of the riser and seawater, respectively, A_r and A_i are the cross-section area and the inner side area of the riser, respectively, x and t are the independent spatial and time variables, respectively and $y(x, t)$ is the lateral displacement of the riser. The potential energy E_p

$$E_p = \int_0^L \left[\frac{1}{2} EI\left(\frac{\partial^2 y}{\partial x^2}\right)^2 + \frac{1}{2} T(x) \left(\frac{\partial y}{\partial x}\right)^2 \right] dx, \tag{2}$$

where E is the Young's modulus of the riser, I is the rotational inertia of the riser cross-section and $T(x)$ is the axial tension of the riser at position x. As mentioned previously, the axial tension includes the self-weight of the riser and BOPs/LMRP, and buoyancy force of the riser. Thus, $T(x)$ can be obtained by [30]

$$T(x) = \left[m_e + (\rho_r - \rho_a) A_r (L - x) \right] g \tag{3}$$

where m_e stands for the mass of BOPs/LMRP, and g is the gravitational acceleration. The virtual work W done by the distributed lateral force and damping force is

$$W = \int_0^L \left[f(x, t)y - c\frac{\partial y}{\partial t} y \right] dx, \tag{4}$$

where $f(x, t)$ is the distributed lateral force and c is the distributed viscous damping coefficient of the riser. Substituting Eq. (1), (2) and (4) into the extended Hamilton's principle and applying the variation operation leads to

$$\int_{t_1}^{t_2} (\delta E_k - \delta E_p + \delta W) dt = 0 \tag{5}$$

Thus, the governing equation can be obtained from Eq. (5), expressed as follows:

$$(\rho_r A_r + \rho_a A_i) \frac{\partial^2 y}{\partial t^2} + c\frac{\partial y}{\partial t} - \frac{\partial}{\partial x}\left[T(x)\frac{\partial y}{\partial x}\right] + EI\frac{\partial^4 y}{\partial x^4} = f(x, t) \tag{6}$$

According to the mechanical model, the boundary conditions of Eq. (6) are

$$y\big|_{x=0} = 0, \quad \frac{\partial y}{\partial x}\Big|_{x=0} = 0, \quad \frac{\partial^2 y}{\partial x^2}\Big|_{x=L} = 0,$$
$$\frac{\partial^3 y}{\partial x^3}\Big|_{x=L} = T(x)\frac{\partial y}{\partial x}\Big|_{x=L} + m_e \frac{\partial^2 y}{\partial t^2}\Big|_{x=L} \tag{7}$$

Zhu [5] proposed a modified form of the Morison equation to describe the lateral force generated by the sea wave and sea current, which includes the relative velocities and accelerations of the seawater and the marine riser. The lateral force that contains the drag force $f_D(x, t)$ and inertial force $f_I(x, t)$ caused by the sea wave and sea current can be expressed as [6]

$$f(x, t) = f_D(x, t) + f_I(x, t) \tag{8}$$

The drag force and inertial force are given by

$$f_D(x, t) = \frac{2C_D}{\pi D}\rho_a A_o (v - \frac{\partial y}{\partial t})|v - \frac{\partial y}{\partial t}| + \frac{2C_D}{\pi D}\rho_a A_o v^2, \tag{9}$$

$$f_I(x, t) = C_M \rho_a A_o \frac{dv_w}{dt} - C_m \rho_a A_o \frac{\partial^2 y}{\partial t^2}, \tag{10}$$

where C_D is the drag coefficient; C_M is the inertial coefficient and $C_m = C_M - 1$; D is the outer diameter of the riser; A_0 is the outer side area of the riser; $v = v_w + v_c$, v_w and $\frac{dv_w}{dt}$ are the sea wave horizontal velocity and its acceleration, respectively; v_c is the sum of the sea current and sea surface wind velocity. According to the Airy wave theory [5], the horizontal velocity of the sea wave in deep water can be obtained as follows:

$$v_w = \frac{\pi H}{T} e^{-kx} \cos(ky - \frac{2\pi}{T} t), \tag{11}$$

where H is the wave height, T is the wave period, k is the wave number, which can be calculated by $k = 2\pi/L_w$, L_w refers to the wave length, which can be obtained using $L_w = T^2 g/2\pi$. A small difference can be observed in the velocity distribution between this work and those by Zhu [5], which is the negative sign in front of the wave number k in Eq. (11). The origin of the coordinate by Zhu [5] is at the sea surface and the direction of the x axis is opposite to gravity, such that the value of x is negative. In this paper, the direction of the x axis is in accordance with gravity, and thus a negative sign should be indicated in front of the wave number k in Eq. (11). The approximate expression of the sea current velocity is given according to the equation recommended by the American Bureau of Shipping [35] as follows:

$$v_c = v_1 (1 - \frac{x}{L_{all}})^{\frac{1}{7}} + v_2 (1 - \frac{x}{L_{all}}), \tag{12}$$

where v_1 and v_2 in Eq. (12) are the sea surface wind velocity and sea surface current velocity, respectively and L_{all} is the total depth of the seawater.

Galerkin's method is applied to calculate the dynamic behaviours of the marine riser. The mechanical model is regarded as a cantilevered Euler–Bernoulli beam, and thus eigenfunctions of a cantilevered beam can be adopted to discretise the governing equations. Suppose $\varphi_j(x)$ is the jth eigenfunction of the cantilevered beam and $q_j(t)$ are the generalised coordinates, then

$$y(x, t) = \sum_{j=1}^{N} \varphi_j(x) q_j(t) \tag{13}$$

and

$$\varphi_j(x) = \frac{1}{\sqrt{L}}\left\{ cosh(\lambda_j \frac{x}{L}) - cos(\lambda_j \frac{x}{L}) - \frac{cosh\lambda_j + cos\lambda_j}{sinh\lambda_j + sin\lambda_j}\left[sinh(\lambda_j \frac{x}{L}) - sin(\lambda_j \frac{x}{L}) \right] \right\} \tag{14}$$

where N is the number of truncating modes taken into the calculations and λ_j is the jth eigenvalue of the cantilevered beam. Substituting Eq. (13) into the governing equation (6) and boundary conditions (7), multiplied by $\varphi_i(x)$ and integrating along the riser axis, leads to

$$m_{ij}\ddot{q}_j + c_{ij}\dot{q}_j + k_{ij} q_j + f_i(q_j, \dot{q}_j) = 0, \tag{15}$$

where m_{ij}, c_{ij}, k_{ij} are the elements of the mass, damping and stiffness matrix of the system, $f_i(q_j, \dot{q}_j)$ is a column vector whose elements represent the lateral force. The values of these matrix and column vectors can be calculated by

$$m_{ij} = (\rho_r A_r + \rho_a A_i + C_m \rho_a A_0) \int_0^L \varphi_i(x)\varphi_j(x) dx + m_e \int_0^L \varphi_i(x)\varphi_j(x)\delta(x - L) dx, \tag{16}$$

$$c_{ij} = c \int_0^L \varphi_i(x)\varphi_j(x) dx, \tag{17}$$

$$k_{ij} = m_e g \int_0^L \varphi_i(x)\varphi'_j(x)\delta(x - L) dx + (\rho_r - \rho_a) A_r g \int_0^L \varphi_i(x)\varphi'_j(x) dx - m_e g \int_0^L \varphi_i(x)\varphi''_j(x) dx - (\rho_r + \rho_a) A_r g \int_0^L \varphi_i(x)\varphi''_j(x)(L - x) dx + EI \int_0^L \varphi_i(x)\varphi''''_j(x) dx, \tag{18}$$

$$f_i = -\frac{2C_D}{\pi D}\rho_a A_o \int_0^L \varphi_i(x)\left(v_w - \frac{\partial y}{\partial t}\right)\left|v_w - \frac{\partial y}{\partial t}\right| dx - \frac{2C_D}{\pi D}\rho_a A_o \int_0^L \varphi_i(x) v_c^2 dx - C_M \rho_a A_o \int_0^L \varphi_i(x)\dot{v}_w dx \quad (19)$$

Eq. (15) can be rewritten in the form that can be programmed using the fourth-order Runge–Kutta method, as is used by Ni et al. [36]. The high-order vibration mode has the characteristic of strong attenuation, and thus, in this paper, the first six modes are applied to approximate the lateral displacement of the riser [8, 31]. The lateral displacement, deformation and Von Mises stress can be obtained. The Von Mises stress can be expressed as

$$\sigma_{von} = \sqrt{\frac{((\sigma_1 - \sigma_2)^2 + (\sigma_2 - \sigma_3)^2 + (\sigma_3 - \sigma_1)^2)}{2}}, \quad (20)$$

where σ_1, σ_2, σ_f from axial tension and positive bending stresses. Thus, the Von Mises stress equals the tensile stress, which is the resultant force of the axial tension stress generated by the self-weight of the riser and BOPs/LMRP, the buoyancy force and the axial bending stress generated by the bending of the riser. The maximum positive bending stress can be used to reflect the stress state of the riser. The mathematical form of the Von Mises stress for the riser can be expressed as follows:

$$\sigma_{von}(x) = \sigma_1 = \frac{T(x)}{A_r} + \frac{1}{2}\frac{M_y(x,t)}{I}D, \quad (21)$$

where $M_y(x, t)$ is the bending moment as a function of time and axis along the riser.

RESULTS AND DISCUSSION

PRACTICAL PROBLEM DESCRIPTION

The parameters of the seawater and riser are given in Table 1. The values of these parameters are constant if not mentioned separately. It must be noted that this is one of the load cases in the actual installation process according to Zhu [5]. In this paper, it represents an analytical calculation of the dynamics of the marine riser in the installation process. The mathematical and analysing schemes may be helpful for other installation environments.

Tab. 1. Parameters for numerical simulation

C_D	0.5	L_{all}	1500 m
C_M	1.5	m_e	200 T
c	0.2	T	13 s
D	0.5334 m	v_1	0.6 m/s
d_t	0.015875 m	v_2	0.3 m/s
E	206 GPa	ρ_a	1030 kg/m^3
g	9.8 m/s^2	ρ_r	7850 kg/m^3
H	15 m		

If the terms related to time are neglected in Eq. (11) and superposed by Eq. (12), the distributions of seawater velocity in the shoal and deep water in the vertical direction are as shown in Fig. 2. The figure shows that if the riser is installed in shoal water, the dynamics of the riser are dominated by the sea wave. The riser will oscillate back and forth with the sea wave. If the riser is installed in deep water, it is influenced mainly by the sea current. In this case, however, part of the riser is still immersed in shoal water. The dynamics of this segment of the riser are dominated by the sea wave.

NUMERICAL VALIDATION

The mathematical model and numerical scheme will be validated in this section. The water depth and weight of the BOPs/LMRP are selected as the parameters. Wang et al. [8] investigated the dynamics of the installation process of marine risers under various water depths, riser lengths and sea water parameters. The lateral displacements of the riser are calculated via the mode superposition method. The vibration modes are assumed as a set of sinusoidal functions that correspond to the boundary conditions of the riser.

In this paper, the equations of motion of the riser are discretised via Galerkin's scheme. The eigenfunctions of a cantilevered beam are adopted, which correspond to the

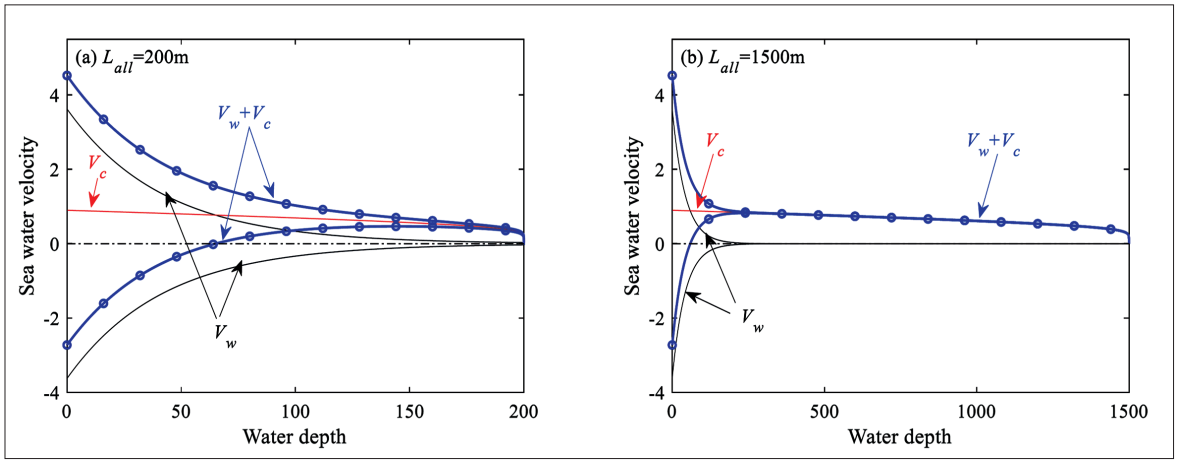

Fig. 2. Distribution of seawater velocity in the vertical direction: (a) shoal water; (b) deep water

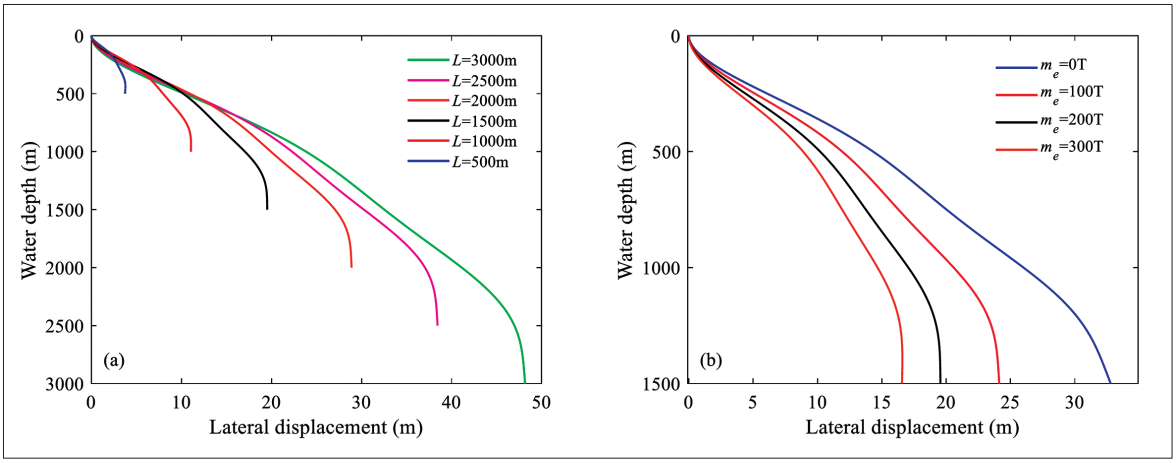

Fig. 3. Maximum lateral vibration displacement with (a) water depth and (b) weight of BOPs/LMRP

boundary conditions of the riser. The maximum lateral displacements of the riser are calculated and compared with those in [8] by changing the values of the water depth and weight of BOPs/LMRP, as shown in Fig. 3. It can be easily observed that the shapes of the riser under the calculating load cases are in qualitative agreement with Fig. 4 and Fig. 6 by Wang et al. [8], except that the values show some discrepancies. This demonstrates the validation of the mathematical model and numerical scheme, which will be used in the following analysis.

INSTALLATION IN SHOAL WATER

As is discussed earlier, the behaviours of seawater in shoal water are different from those in deep water. The influence of the sea surface wind and current flow is relatively small. The lateral force is generated mainly by the wave. Hence, the riser's vibration is forced back and forth following the oscillation of the sea waves. According to the parameters, the period of the sea wave is 13 s, which is also the frequency of the forced vibration of the riser induced by the sea wave. The amplitude of the first six truncating modes may differ with various lengths. Fig. 4 presents the maximum displacement of the riser at three values of the length of the riser. L = 80 m and L = 150 m are

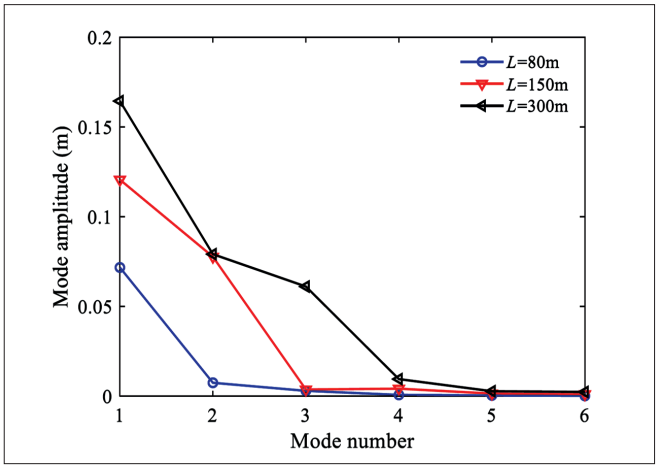

Fig. 4. Maximum displacement of the first six modes at x = L

in the range of shoal water and L = 300 m can be seen as the transition from shoal water to deep water, whose behaviour can be explained with the same scheme as that in shoal water. It can be inferred from Fig. 4 that the marine riser vibrates mainly in its first mode with L = 80 m; with L = 150 m, the riser oscillation is dominated by its first two modes. For the case of L = 300 m, the vibration consists of the first three modes. From this point of view, for numerical simulation in shoal water, the first four modes are accurate enough to obtain reliable results.

The responses of the lateral deflection and Von Mises stress in time and space with the lengths of L = 80 m, L = 150 m, and L = 300 m are presented in Fig. 5. The vibration mode can be observed through the deflection of the riser with various lengths, and the performance of Von Mises stress along the riser can also be observed. The tip of the riser ($x = L$), which is connected by BOPs/LMRP, has the maximum displacement and vibrates periodically in a specific behaviour as depicted by Fig. 6. The offset and vibration amplitude at $x = L$ are listed in Table 2.

Tab. 2. Offset and vibration amplitude at x=L with various lengths of the riser

Riser length	L = 80 m	L = 150 m	L = 300 m
Offset (m)	0.1342	0.4918	1.8055
Vibration amplitude (m)	0.3975	0.1818	0.1335

Fig. 5 implies that the stress concentration position occurs at the clamped end ($x = 0$), which varies with the oscillation of the riser. This means that at the clamped end, the Von Mises stress is affected mainly by the bending moment. The other part of the riser is subjected to axial extension and tension stresses generated by the bending moment. The time trace of the maximum Von Mises stress at the clamped end is shown in Fig. 7. According to the DNV-OS-F101 standard [37], the material of the offshore drilling riser is API 5L X80 pipeline steel and the minimum yield strength is 555 MPa, which means that, for this paper, the riser installation process is safe enough. If the load cases are more complicated and adverse, the offset and Von Mises stress can be obtained through the scheme used in this paper.

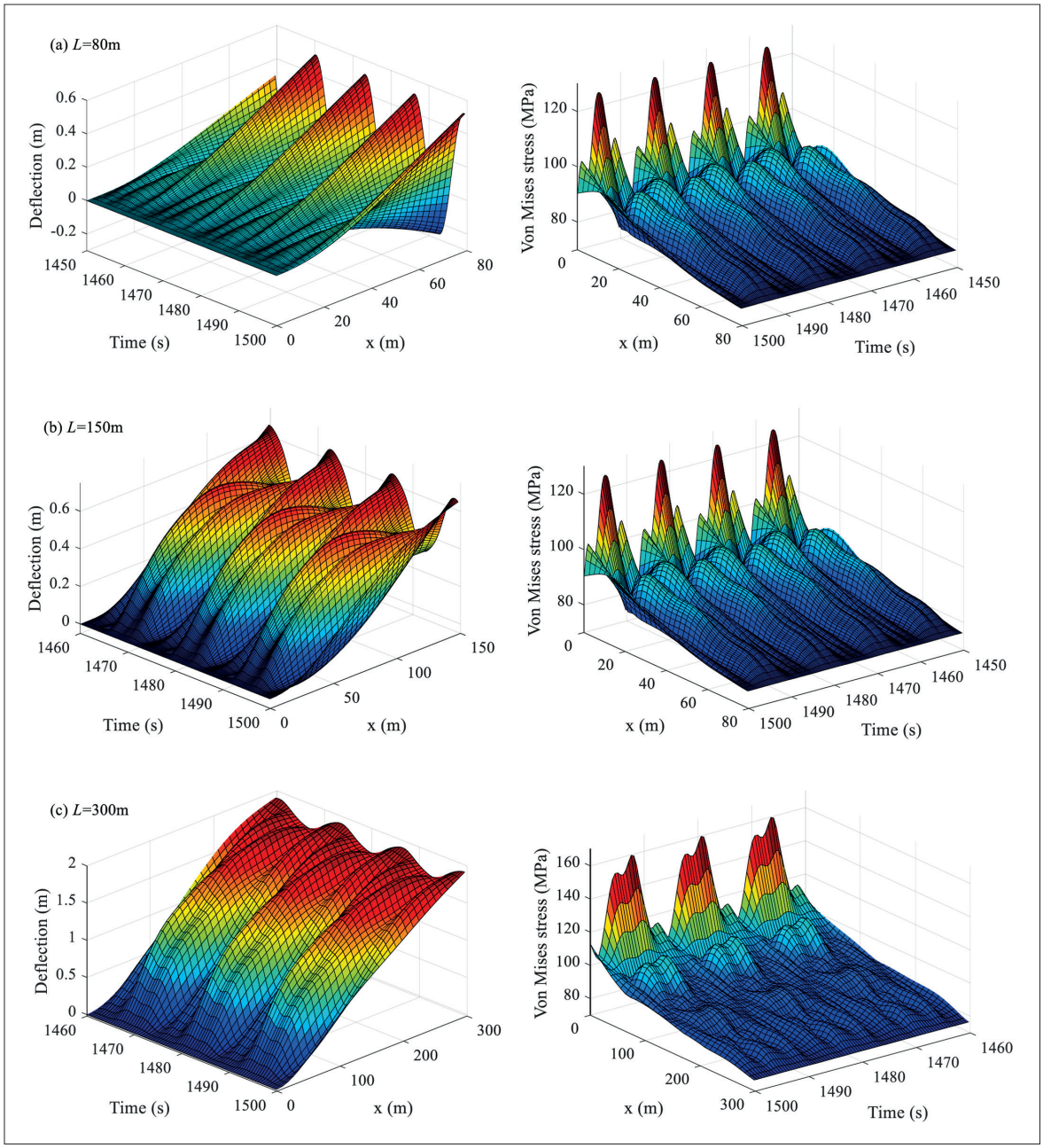

Fig. 5. Deflections and Von Mises stresses during the installation in shoal water

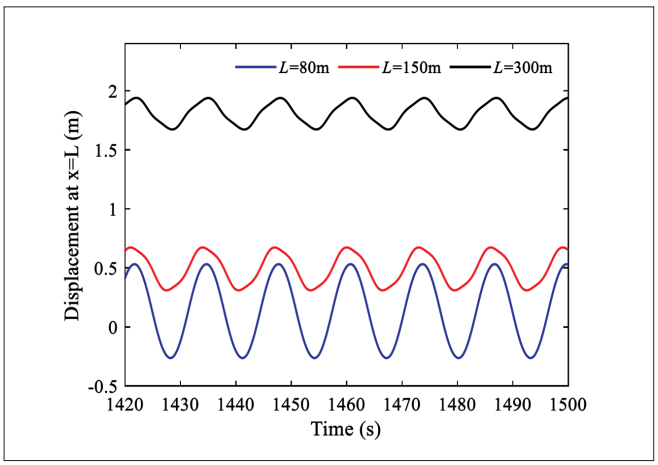

Fig. 6. Time trace of displacement at x = L

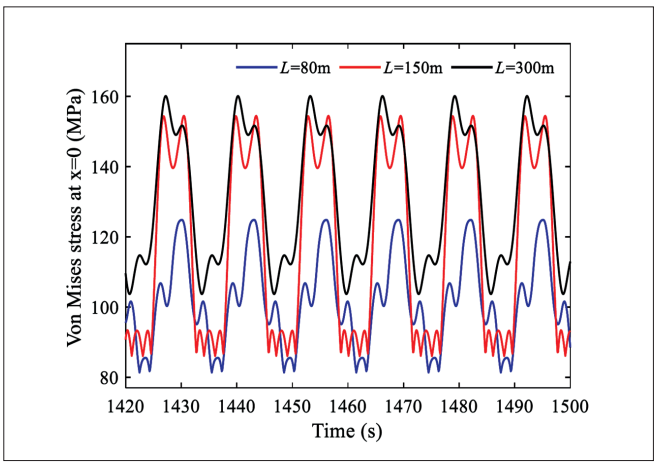

Fig. 7. Time trace of Von Mises stress at x = 0

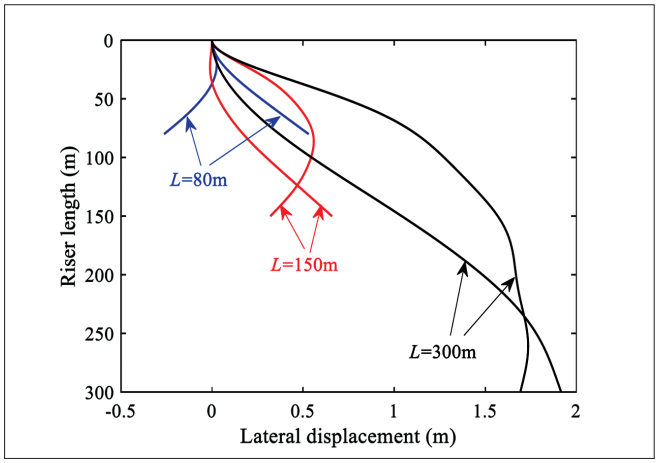

Fig. 8. Riser shape for maximum and minimum Von Mises stress at x = 0

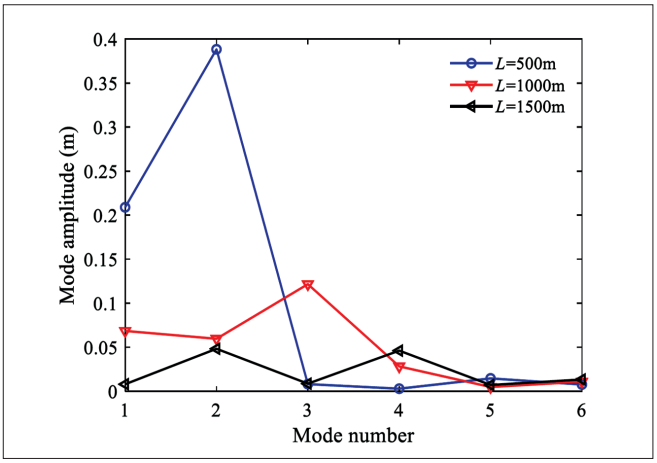

Fig. 9. Maximum displacement of the first six modes at x = L

The vibration shapes in the installation process for the maximum and minimum Von Mises stress at the clamped end are shown in Fig. 8. The deflections of the riser for the three lengths exhibit considerable differences. The first mode dominates for the case of L = 80 m as can be seen in Fig. 8. When the length of the riser increases to L = 150 m, the second mode deflection takes part in the flow-induced vibration. The offset of the riser is larger than those with L = 80 m. With the length increasing to L = 300 m, the stiffness is significantly less than the risers with a short length. Hence, the offset of the riser with L = 300 m is much larger than those with a smaller length. Higher modes of deflection can be observed in Fig. 8.

INSTALLATION IN DEEP WATER

Let us change our view to the case of installation in deep water. As depicted in Fig. 2(b), the velocity of the seawater is dominated by the sea surface wind and sea current. If the riser is installed in deep water, the clamped end of the riser is affected by the sea wave and the lower end of the riser is affected by the sea surface wind and sea current. The lateral force is a periodic force in the shoal water and a steady force in deep water. From this perspective, the behaviours of the riser consist of a steady deflection and a small amplitude vibration superposed on the steady deflection. Under this load case, the contribution of the first six modes is expressed in Fig. 9. For , the dynamics of the riser is influenced mainly by the first and second modes. For , the first four modes show high involvement in its vibration, and the third mode is the most significant one. For , the second and fourth modes dominate the dynamics of the riser.

The lateral deflection and Von Mises stress distribution in time and space are illustrated in Fig. 10. The frequency and amplitude of vibration decrease with the increase of the riser length, but the values of the Von Mises stress increase with the increase of length. The variation of the Von Mises stress is smaller and smaller in time and space. It can be explained in this way: Eq. (6) shows that the self-weight of the riser has a large influence on the dynamics of the riser. The inertial force of the system in the vertical and lateral directions increases because the riser is very long. The behaviours of the riser in deep water are affected mainly by the sea surface wind and sea current. The effects of the sea wave can be neglected in deep water. Thus, the deflection and Von Mises stress become increasingly stable as the riser becomes increasingly long.

Time traces of the displacement at $x = L$ and Von Mises stress at x = 0 are shown in Fig. 11 and 12, respectively. The time traces differ slightly compared with Fig. 6 and 7. In deep water, due to the existence of drag force generated by the sea surface wind and sea current, the riser is dragged downstream of the sea current. At the same time, the part of the riser in the shoal water is forced into vibration by the sea wave, and this behaviour is transmitted along the riser axis. Thus, we can see in Fig. 11 that the tip of the riser vibrates at a small amplitude. The offset and vibration amplitude at $x = L$ are listed in Table 3. The lateral displacements of the riser installed in deep water are obviously larger than those installed in shoal water, as shown in Table 2. However, the vibration amplitudes in deep water are smaller than those installed in shoal water. It can be explained that the fluctuation fluid forces induced by the sea wave are more severe than the drag force induced by the sea current when installed in deep water, while in deep water the effect of the drag force is more obvious than the fluctuation fluid forces. From this point, when the riser is installed in the stage of shoal water, the offset at $x = L$ is smaller and the vibration amplitude is larger than those installed in deep water.

Fig. 12 gives the time trace of Von Mises stress at x = 0, from which the maximum and minimum stress of the riser can be obtained. According to the DNV-OS-F101 standard [37], the riser installation process is safe enough in the case of installation in deep water.

Tab. 3. Offset and vibration amplitude at x=L with various lengths

Riser length	L = 500 m	L = 1000 m	L = 1500 m
Offset (m)	4.255	10.945	14.44
Vibration amplitude (m)	0.327	0.175	0.07

The vibration shapes in the installation process for the maximum and minimum Von Mises stress at the clamped end are shown in Fig. 13. The responses differ from those of a riser installed in shoal water. The offset of the riser is much

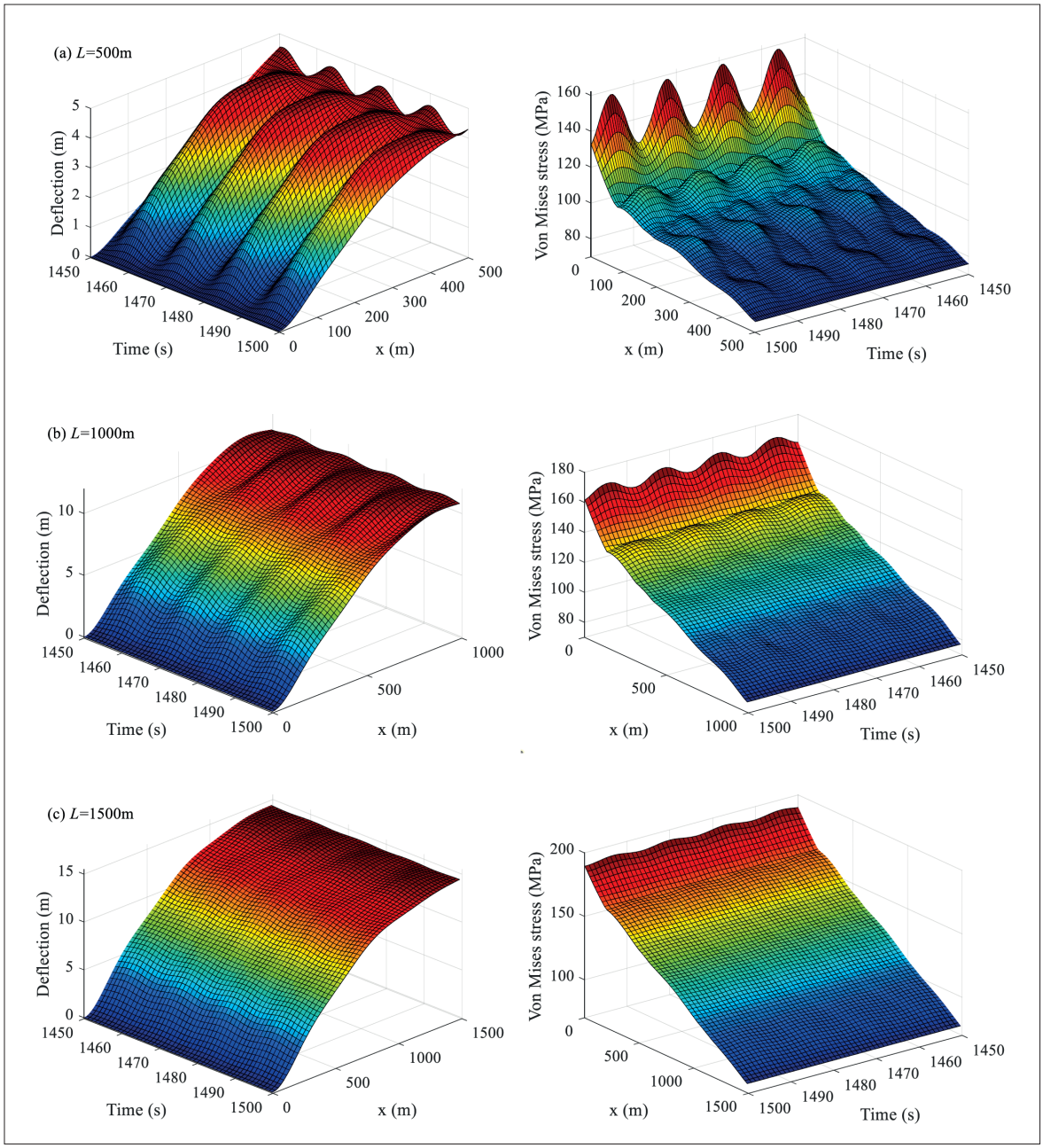

Fig. 10. Deflections and Von Mises stresses during the installation in deep water

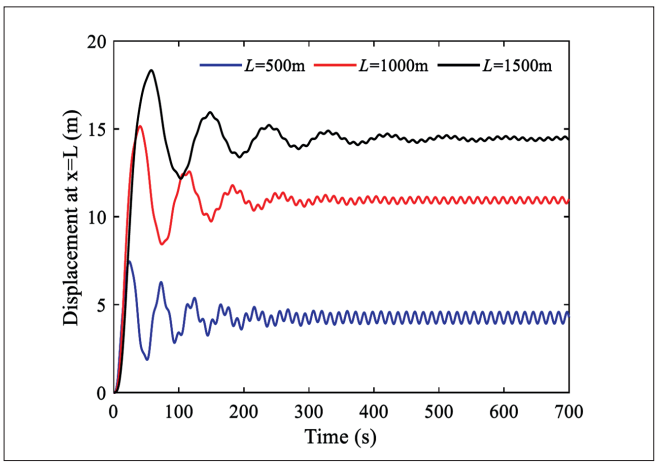

Fig. 11. Time trace of displacement at x = L

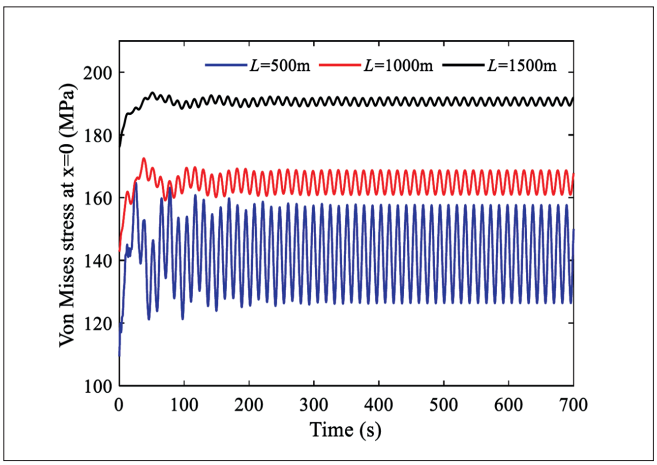

Fig. 12. Time trace of Von Mises stress at x = 0

larger, while the vibration amplitude is much smaller compared with the risers installed in shoal water. This difference can be explained by the dragging force generated by the sea current acting on the riser installed in deep water, which is dominated by the sea current, instead of the sea wave, which exhibits a quasi-static force. Hence, the small periodic exciting force generated by the sea wave introduces a small vibration amplitude of the riser in deep water.

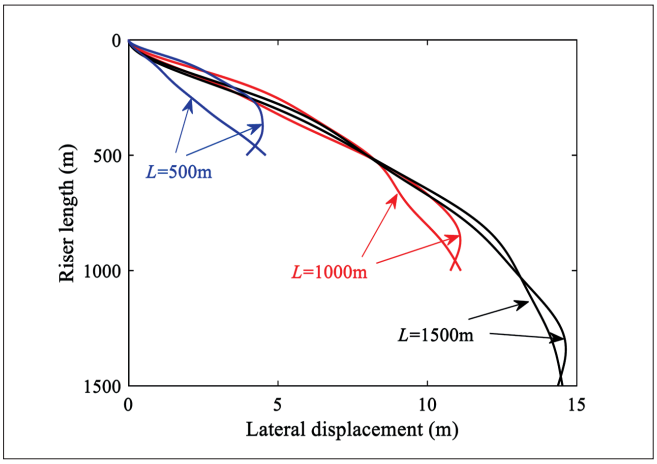

Fig. 13. Riser shape for maximum and minimum Von Mises stress at x = 0

CONCLUSIONS

The mechanics of a marine riser in an installation subjected to shoal water and deep water is discussed in this paper. The mathematical model is considered as a cantilevered Euler–Bernoulli beam clamped on a fixed vessel or drilling platform. The riser suffers from the axial extension force induced by the self-weight of the riser and BOPs/LMRP, and the buoyancy forces of the riser, as well as lateral fluid forces generated by the seawater. Considering the two types of external force, equations of motion and boundary conditions are derived via the variation approach. Galerkin's scheme and fourth-order Runge–Kutta integrating method are adopted to discretise and solve the governing equations.

The velocity distribution of the seawater is depicted in shoal water and deep water. The results show that the effect of sea waves is more obvious in shoal water. In deep water, sea surface wind and sea current velocity are more significant in the installation process. In shoal water, the lateral force is dominated by the sea wave, such that periodicity is obvious. The riser is forced by the sea wave into vibrating back and forth. The deflection and Von Mises stress also vary periodically with the sea wave. In deep water, the lateral force is influenced by the sea surface wind and sea current velocity. The sea wave effect is weak compared to the two velocities. Under this load case, the participation of higher-order modes is evident, whose vibration amplitude is small. The results of the deflection and Von Mises stress distribution reveal that if the riser is installed in deep water, the oscillating phenomena will decrease with the increase of the riser length. The time traces of tip displacement illustrate that the offset increases and vibration amplitude decreases with a longer marine riser. The results of this paper are helpful to realise safe and quick installation of marine risers.

DATA AVAILABILITY

All data generated or analysed during this study are included in the published article.

CONFLICTS OF INTEREST

The authors declare that there is no conflict of interest regarding the publication of this paper.

ACKNOWLEDGEMENTS

This work was supported by the Scientific Research Project of Education Department of Hubei Province (No. Q20212601).

REFERENCES

1. Y. Wang, L. Wang, Q. Ni, M. Yang, D. Liu, T. Qin (2021): Non-smooth dynamics of articulated pipe conveying fluid subjected to a one-sided rigid stop. Applied Mathematical Modelling, Vol. 89, 802-818.

2. L. Mao, S. Zeng, Q. Liu (2019): Dynamic analysis of soft hang-off riser in deep water, coupling the vibration of lateral and longitudinal directions. Current Science, Vol. 116(9), 1533-1543.

3. J. M. Cabrera-Miranda, J. K. Paik (2017): On the probabilistic distribution of loads on a marine riser. Ocean Engineering, Vol. 134, 105-118.

4. M. Szczotka (2011): Dynamic analysis of an offshore pipe laying operation using the reel method. Acta Mechanica Sinica, Vol. 27(1), 44-55.

5. Y. Zhu. Ocean engineering wave mechanics. Tianjin University Press, 1991.

6. Y. Wang, D. Gao, J. Fang (2015): Mechanical behavior analysis for the determination of riser installation window in offshore drilling. Journal of Natural Gas Science and Engineering, Vol. 24, 317-323.

7. W. He, S. Zhang, S. S. Ge (2013): Boundary control of a flexible riser with the application to marine installation. IEEE Transactions on Industrial Electronics, Vol. 60(12), 5802-5810.

8. Y. Wang, D. Gao, J. Fang (2015): Study on lateral vibration analysis of marine riser in installation-via variational approach. Journal of Natural Gas Science and Engineering, Vol. 22, 523-529.

9. S. K. Chakrabarti (1972): Nonlinear wave forces on vertical cylinder. Journal of the Hydraulics Division, Vol. 98, 1-11.

10. E. Wang (1983): Analysis of two 13,200-ft riser systems using a three-dimensional riser program. In: *Proceedings of the Offshore Technology Conference*, Houston, Texas, USA, 1983.

11. W. Azpiazu, M. Thatcher, E. Schwelm (1983): Heave compensation systems: analysis and results of field testing. In: *Proceedings of the Offshore Technology Conference*, Houston, Texas, USA, 1983.

12. W. Azpiazu, V. Nguyen (1984): Vertical dynamics of marine risers. In: *Proceedings of the Offshore Technology Conference*, Houston, Texas, USA, 1984.

13. A. Trim (1991): Axial dynamics of deep water risers. In: *Proceedings of the The First International Offshore and Polar Engineering Conference*, Edinburgh, The United Kingdom, 1991.

14. C. Johnson, J. Roesset (1992). Axial-bending coupling effects on the dynamic response of deep water risers. In: *Proceedings of the The Second International Offshore and Polar Engineering Conference*, San Francisco, California, USA, 1992.

15. R. Burrows, R. Tickell, D. Hames, G. Najafian (1997): Morison wave force coefficients for application to random seas. Applied Ocean Research, Vol. 19(3), 183-199.

16. G. Moe, B. Larsen (1997): Dynamics of deep water marine risers - asymptotic solutions. In: *Proceedings of the The Seventh International Offshore and Polar Engineering Conference*, Honolulu, Hawaii, USA, 1997.

17. E. Kogure, M. Ohashi, S. Urabe, A. Tanabe (1998): Applications of a near surface disconnectable drilling riser in deepwater. In: *Proceedings of the IADC/SPE Asia Pacific Drilling Technology*, Jakarta, Indonesia, 1998.

18. M. H. Patel, F. B. Seyed (1995): Review of flexible riser modelling and analysis techniques. Engineering Structures, Vol. 17(4), 293-304.

19. C. Athisakul, T. Huang, S. Chucheepsakul (2002): Large strain static analysis of marine risers via a variational approach. *Proceedings of the Twelfth International Offshore and Polar Engineering Conference*, Kitakyushu, Japan, 2002.

20. M. Yazdchi, M. Crisfield (2002): Non-linear dynamic behaviour of flexible marine pipes and risers. International Journal for Numerical Methods in Engineering, Vol. 54(9), 1265-1308.

21. W. Raman-Nair, E. Baddour (2003): Three-dimensional dynamics of a flexible marine riser undergoing large elastic deformations. Multibody System Dynamics, Vol. 10, 393-423.

22. L. Mathelin, E. de Langre (2005): Vortex-induced vibrations and waves under shear flow with a wake oscillator model. European Journal of Mechanics - B/Fluids, Vol. 24(4), 478-490.

23. I. K. Chatjigeorgiou (2008): A finite differences formulation for the linear and nonlinear dynamics of 2D catenary risers. Ocean Engineering, Vol. 35(7), 616-636.

24. W. Dai, F. Gao, Y. Bai (2009): FEM analysis of deepwater drilling risers under the operability and hang-off working conditions. Journal of Marine Science and Application, Vol. 8(2), 156-162.

25. S. T. Santillan, L. N. Virgin, R. H. Plaut (2010): Static and dynamic behavior of highly deformed risers and pipelines. Journal of Offshore Mechanics and Arctic Engineering, Vol. 132(2), 021401.

26. S. S. Ge, W. He, B. V. E. How, Y. S. Choo (2010): Boundary control of a coupled nonlinear flexible marine riser. IEEE Transactions on Control Systems Technology, Vol. 18(5), 1080-1091.

27. W. He, X. He, S. S. Ge (2016): Vibration control of flexible marine riser systems with input saturation. IEEE/ASME Transactions on Mechatronics, Vol. 21(1), 254-265.

28. P. Ma, W. Qiu, D. Spencer (2014): Numerical vortex-induced vibration prediction of marine risers in time-domain based on a forcing algorithm. Journal of Offshore Mechanics and Arctic Engineering, Vol. 136(3), 031703.

29. Y. Wang, D. Gao, J. Fang (2014): Axial dynamic analysis of marine riser in installation. Journal of Natural Gas Science and Engineering, Vol. 21, 112-117.

30. Y. Wang, D. Gao, J. Fang (2014): Static analysis of deep-water marine riser subjected to both axial and lateral forces in its installation. Journal of Natural Gas Science and Engineering, Vol. 19, 84-90.

31. Y. Wang, D. Gao, J. Fang (2015): Study on lateral nonlinear dynamic response of deepwater drilling riser with consideration of the vessel motions in its installation. Tech Science Press, Vol. 48(1), 57-75.

32. Y. Hu, B. Yao, Z. Zheng, L. Lian (2016): Research on marine riser in different installations stages of subsea production tree. In: *Proceedings of the OCEANS 2016-Shanghai*, Shanghai, China, 2016: 1-7.

33. X. Chang, J. Fan, W. Yang, Y. Li, R. Kolahchi (2021): In-line and cross-flow coupling vibration response characteristics of a marine viscoelastic riser subjected to two-phase internal flow. Shock and Vibration, Vol. 2021, 1-27.

34. M. Liu, Y. Wang, T. Qin, J. Zhao, Y. Du (2021): Nonlinear dynamics of cross-flow tubes subjected to initial axial load and distributed impacting constraints. Shock and Vibration, Vol. 2021, 1-15.

35. Y. Chang, G. Chen, L. Xu, H. Wang (2007): Nonlinear dynamic analysis of deep pipe-in-pipe steel catenary riser. China Offshore Oil and Gas, Vol. 3(19), 203-206.

36. Q. Ni, Y. K. Wang, M. Tang, Y. Y. Luo, H. Yan, L. Wang (2015): Nonlinear impacting oscillations of a fluid-conveying pipe subjected to distributed motion constraints. Nonlinear Dynamics, Vol. 81(1-2), 893-906.

37. Det Norske Veritas (2000): Offshore standard DNV-OS-F101. Submarine pipeline systems, 45-78.

CONTACT WITH THE AUTHORS

Yikun Wang
e-mail: wangyikun18@hbuas.edu.cn

Songxiang Luo
e-mail: 2534203508@qq.com

Mo Yang
e-mail: ym901116@163.com

Tao Qin
e-mail: heu_qt@163.com

Jing Zhao
e-mail: zhaojing@hbuas.edu.cn

Gang Yu
e-mail: yugang@hbuas.edu.cn

School of Mechanical Engineering
Hubei University of Arts and Science
Longzhong Street, 441053 Xiangyang City
China